

**Figure 2.** (A) First-order constant for  $O_2(^1\Delta_g)$  luminescence decay,  $k'$ , as a function of radiation dose for an aerated hexadeuteriobenzene solution of 2-acetonaphthone ( $2 \times 10^{-2} \text{ mol L}^{-1}$ ). The data point at zero dose corresponds to  $k'$  determined after pulsed laser excitation (355 nm; 1 mJ) of an identical solution (cf. ref 10a,c, 13a,c). Inset: corresponding transient luminescence, with first-order fit, after absorption of a 3.65-Gy electron pulse: 20 mV/division, 100  $\mu\text{s}$ /division,  $k' = 3.6 \times 10^3 \text{ s}^{-1}$ . (B) Relative  $O_2(^1\Delta_g)$  luminescence yields, measured as mV of deflection and extrapolated to time zero, as a function of radiation dose for sensitizers ( $2 \times 10^{-2} \text{ mol L}^{-1}$ ) in aerated hexadeuteriobenzene: (a) naphthalene and (b) benzophenone. A small correction for the effects of  $\phi_{\text{isc}}$  on  $G$  values gave a ratio of slopes of 1.7, to be compared with a published value of 1.9 for benzene.<sup>8c</sup> Inset: corresponding transient luminescence, with first-order fit, after absorption of a 6.65-Gy electron pulse with naphthalene as sensitizer: 50 mV/division, 100  $\mu\text{s}$ /division.

efforts in this direction have proved fruitless due to (a) a non-light-induced signal resulting from bombardment of the germanium detector by scattered X-rays and (b) an intense IR signal due to Čerenkov emission.<sup>16</sup> Both signals were orders of magnitude higher in intensity than that anticipated for  $O_2(^1\Delta_g)$  emission. Such problems have been overcome as detailed below.

The reaction cell and germanium detector were physically separated while remaining "close-coupled" by means of a 7-m length of fiber optic cable.<sup>18</sup> This allowed the detector to be situated outside the concrete-enclosed, radiation-exposed area, and the resultant loss of the scattered X-ray effect is demonstrated in Figure 1 (parts A and B). When, with this detection configuration, an aerated solution of a sensitizer, e.g., 2-acetonaphthone ( $2 \times 10^{-1} \text{ mol L}^{-1}$ ), in benzene ( $\tau_{\Delta} \sim 33 \mu\text{s}$ )<sup>13e</sup> was subjected to a 100-ns pulse of 10 MeV electrons, the  $O_2(^1\Delta_g)$  emission signal was virtually indiscernible from the detector response to the

Čerenkov emission. However, as demonstrated in Figure 1 (parts C and E), the same experiment repeated in hexadeuteriobenzene ( $\tau_{\Delta} 550\text{--}700 \mu\text{s}$ )<sup>10a,c,13a,c</sup> allowed clear time resolution of the two signals. The  $O_2(^1\Delta_g)$  emission signal from a *single shot* experiment (Figure 1E) had excellent signal-to-noise characteristics with an intensity which compared favorably to that observed on pulsed laser excitation at 355 nm ( $\sim 1 \text{ mJ}$  per pulse) of 2-acetonaphthone ( $\text{OD}_{355} = 1.0$ ) in aerated benzene with cell and detector physically close-coupled.<sup>19</sup>

Several independent controls have unequivocally identified the "slow" emission of Figure 1E as that corresponding to eq 6.

(i) It disappeared completely on deaeration, but the fast Čerenkov spike was unchanged (cf. Figure 1 (parts C–F)).

(ii) Its strictly exponential decay (Figure 1E) was, as diagnosed previously for  $O_2(^1\Delta_g)$ ,<sup>3</sup> linearly dependent on radiation dose (Figure 2A). Extrapolation to zero dose and zero sensitizer concentration gave a lifetime of 625  $\mu\text{s}$ , in excellent agreement with published  $\tau_{\Delta}$  values for hexadeuteriobenzene.<sup>10a,c,13a,c</sup>

(iii) Its yield, extrapolated to time zero, was sensitizer dependent (Figure 2B). The relative values for benzophenone and naphthalene were essentially identical with those recently measured in benzene.<sup>8c</sup>

(iv) Its decay rate was enhanced by the efficient  $O_2(^1\Delta_g)$  quencher strychnine. The routinely determined rate constant,  $8.8 \times 10^8 \text{ L mol}^{-1} \text{ s}^{-1}$ , was essentially identical with that already reported for benzene,  $9.0 \times 10^8 \text{ L mol}^{-1} \text{ s}^{-1}$ .<sup>20</sup>

**Acknowledgment.** Experiments were performed at the Paterson Institute for Cancer Research. Support for this work came from SERC Grant 52169 and the Cancer Research Campaign.

**Registry No.**  $O_2$ , 7782-44-7; Ge, 7440-56-4;  $C_6D_6$ , 1076-43-3; strychnine, 57-24-9; benzophenone, 119-61-9; naphthalene, 91-20-3; 2-acetonaphthone, 93-08-3.

(19) The Čerenkov emission follows the electron beam profile and only appears as a "slow" signal due to the risetime of the detection system.<sup>15</sup> Current experimentation is aimed at effectively grounding the diode current for several hundreds of nanoseconds followed by rapid switching of the normal load resistance into the circuitry. This is a nontrivial exercise with diodes but, if successful, will remove the problem of the Čerenkov-derived signal and allow examination of solvents with short  $\tau_{\Delta}$  values, including benzene itself.

(20) Gorman, A. A.; Hamblett, I.; Smith, K.; Standen, M. C. *Tetrahedron Lett.* 1984, 25, 581.

### Preparation of a Discrete, Closed-Transition-Metal Boride. Characterization and Structure of *trans*-[Fe<sub>4</sub>Rh<sub>2</sub>(CO)<sub>16</sub>B]PPN

Rajesh Khattar, Jose Puga, and Thomas P. Fehlner\*

Department of Chemistry, University of Notre Dame  
Notre Dame, Indiana 46556

Arnold L. Rheingold\*

Department of Chemistry, University of Delaware  
Newark, Delaware 19716

Received September 28, 1988

Transition-metal main-group solid-state compounds, e.g., carbides, are important materials.<sup>1</sup> The simplest compounds can be viewed as a metal lattice with individual main-group atoms in a set of interstitial holes. There are well-known examples of discrete molecular clusters containing electron precise (H and group 14)<sup>2</sup> or electron rich (groups 15<sup>3</sup> and 16<sup>4</sup>) interstitial atoms.

(1) Greenwood, N. N.; Earnshaw, A. *Chemistry of the Elements*; Pergamon Press: New York, 1984; p 162.

(15) The detection system used previously has been described.<sup>13f,8c</sup> Points to be emphasized are as follows: (a) Reaction cell and germanium detector must be close-coupled. (b) A silicon filter cuts out incident light below 1100 nm. (c) The requisite sensitivity leads to a detection system risetime of  $\sim 500$  ns. (d) Single shot experiments with laser energies of  $\geq 0.2 \text{ mJ}$  at 355 nm lead to acceptable signal-to-noise ratios, for efficient  $O_2(^1\Delta_g)$  formation, with deflection sensitivities of  $\geq 2 \text{ mV/division}$ . (e) Amplifier saturation occurs with emission-derived signals corresponding to slightly more than 1 V of deflection.

(16) Čerenkov emission is a consequence of the retardation of electrons which enter a medium with a velocity higher than that of light in that medium. In the context of our experiments both the cell glass (Spectrosil) and the solvent are involved.<sup>17</sup>

(17) Jelley, J. V. *Čerenkov Radiation and Its Applications*; Pergamon Press: London, 1958.

(18) The 10-mm cable was supplied by Optronics Ltd., Cambridge, U.K. The  $\sim 50 \mu\text{m}$  diameter fibers were of silica, and the light loss per meter was 15%.

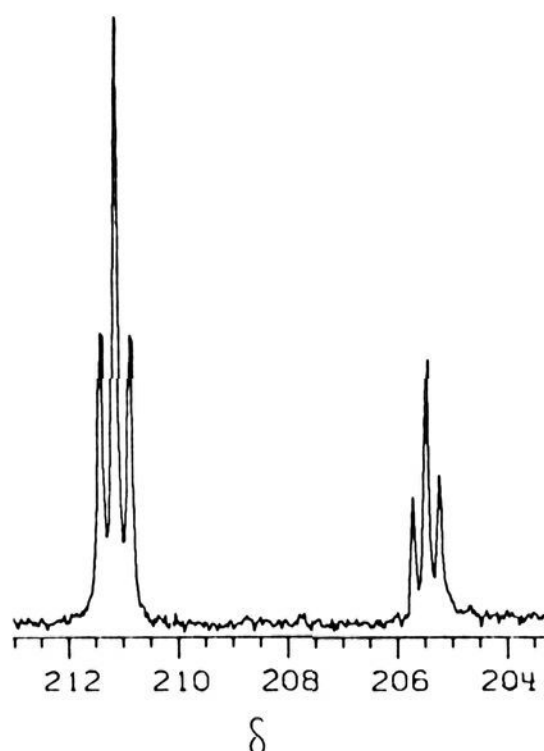


**Figure 1.**  $^{11}\text{B}$  NMR spectrum of a mixture of *cis*- $[\text{Fe}_4\text{Rh}_2(\text{CO})_{16}\text{B}]^-$  and *trans*- $[\text{Fe}_4\text{Rh}_2(\text{CO})_{16}\text{B}]^-$  the latter being most abundant. Chemical shift shown is relative to  $\delta = 0$  for  $\text{BF}_3\cdot\text{OEt}_2$ .

Solid-state metal borides are also important materials, and their properties and structures have been reported in detail.<sup>1,5</sup> These substances exhibit a variety of structural types containing periodic units of one or several boron atoms. Hence, a discrete, closed-transition-metal boride constitutes an attractive synthetic goal.<sup>6</sup>

We have noted the boridic nature of the boron atom in  $\text{H-Fe}_4(\text{CO})_{12}\text{BH}_2$  (**1**).<sup>7</sup> This molecule has been successfully deprotonated to form the anion  $[\text{Fe}_4(\text{CO})_{12}\text{B}]^{3-}$  which is an example of a metal cluster containing an exposed boride and one iso-electronic with  $[\text{Fe}_4(\text{CO})_{12}\text{C}]^{2-}$ .<sup>8,9</sup> Replacement of the protons of **1** with  $[\text{AuPR}_3]^+$  cations leads to compounds such as  $\text{Fe}_4(\text{CO})_{12}(\text{AuPR}_3)_3\text{B}$  or  $\text{HFe}_4(\text{CO})_{12}(\text{AuPR}_3)_2\text{B}$  which contain a boron atom interacting only with metal atoms.<sup>10</sup> Although these gold derivatives of **1** are formally borides, the  $[\text{AuPR}_3]^+$  fragment is isolobal with  $\text{H}^+$  and primarily uses a single frontier orbital in interacting with another species. Hence, our objective has been to close the open face of **1** with two  $\text{ML}_n$  fragments that utilize three frontier orbitals each in order to produce a true analogue of the solid-state environment as well as a robust species. The search for a closed boride is aided by a correlation between the  $^{11}\text{B}$  chemical shift of metal-rich metallaboranes and the number of direct metal-boron interactions.<sup>11</sup> Species containing boron in a highly metallic environment can be easily distinguished from other types of boron by virtue of extreme low field chemical shifts,

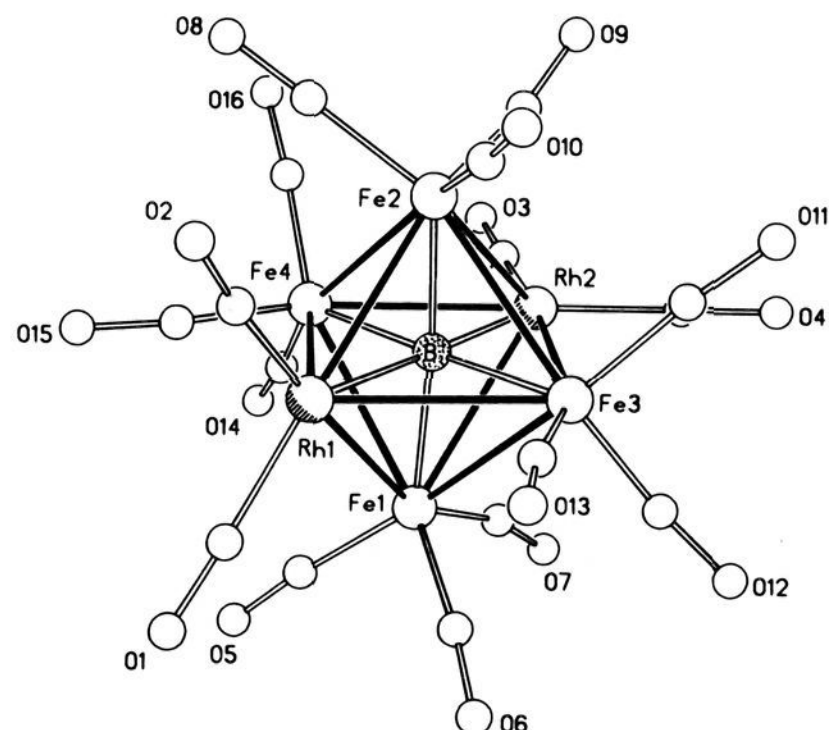
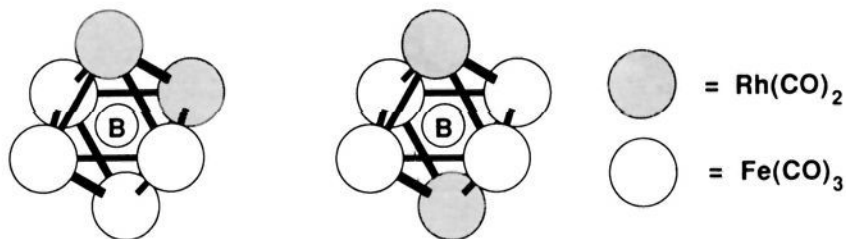


**Figure 2.** Structure of *trans*- $[\text{Fe}_4\text{Rh}_2(\text{CO})_{16}\text{B}]^-$ . Selected bond distances: Rh(1)-Fe(1), 2.719 (1); Rh(1)-Fe(2), 2.719 (2); Rh(1)-Fe(3), 2.914 (2); Rh(1)-Fe(4), 2.834 (2); Rh(2)-Fe(1), 2.907 (1); Rh(2)-Fe(2), 2.881 (2); Rh(2)-Fe(3), 2.740 (2); Rh(2)-Fe(4), 2.743 (2); Fe(1)-Fe(3), 2.748 (2); Fe(1)-Fe(4), 2.763 (2); Fe(2)-Fe(3), 2.748 (2); Fe(2)-Fe(4), 2.748 (2); Rh(1)-B, 2.042 (11); Rh(2)-B, 2.013 (11); Fe(1)-B, 1.935 (9); Fe(2)-B, 1.952 (9); Fe(3)-B, 1.935 (10); Fe(4)-B, 1.951 (10) Å.

#### Chart I



and the number of direct M-B interactions can often be estimated from the correlation.

Although treatment of the anions derived from **1** with a variety of metal fragment sources resulted in no boron-containing metal cluster product, we have been successful utilizing  $[\text{Rh}(\text{CO})_2\text{Cl}]_2$  as a formal source of  $[\text{Rh}(\text{CO})_2]^+$ .<sup>12</sup> The reaction of any of the anions derived from **1**, with 1 mol equiv or excess  $[\text{Rh}(\text{CO})_2\text{Cl}]_2$  proceeds smoothly in THF at 25 °C with the formation of a single final product in high yield (quantitative by  $^{11}\text{B}$  NMR). The course of the reaction has been monitored by  $^{11}\text{B}$  NMR thereby producing evidence for the initial formation of a five metal species which is rapidly (ca. 30 min.) converted into a six metal species<sup>13</sup> followed by a slower (ca. 12 h) conversion into a different six metal species.<sup>14</sup> The anionic mass of the final product corresponds to  $[\text{Fe}_4\text{Rh}_2(\text{CO})_{16}\text{B}]^-$ . The IR spectrum is also consistent with an anionic cluster and is a simple spectrum very similar to that exhibited by  $[\text{Fe}_6(\text{CO})_{16}\text{C}]^{2-}$ .<sup>15</sup> The  $^{11}\text{B}$  NMR spectrum (Figure 1) is definitive. The very low field shift is consistent with a boron atom interacting with four iron and two rhodium atoms.<sup>11</sup> The line width is 12 Hz demonstrating a very symmetrical environment for the boron atom.<sup>16</sup> The very narrow lines allow coupling to

(2) Bradley, J. S. *Adv. Organomet. Chem.* **1983**, *22*, 1 and references therein. Eady, C. R.; Jackson, P. F.; Johnson, B. F. G.; Lewis, J.; Malatesta, M. C.; McPartlin, M.; Nelson, W. J. H. *J. Chem. Soc., Dalton Trans.* **1980**, 383. Mackay, K. M.; Nicholson, B. K.; Robinson, W. T.; Sims, A. W. *J. Chem. Soc., Chem. Commun.* **1984**, 1276.

(3) Ciani, G.; Martinengo, S. *J. Organomet. Chem.* **1986**, *306*, C49. Martinengo, S.; Ciani, G.; Sironi, A.; Heaton, B. T.; Mason, J. *J. Am. Chem. Soc.* **1979**, *101*, 7905. Bonfichi, R.; Ciani, G.; Sironi, A.; Martinengo, S. *J. Chem. Soc., Dalton Trans.* **1983**, 253. Vidal, J. L. *Inorg. Chem.* **1981**, *20*, 243. Vidal, J. L.; Troup, J. M. *J. Organomet. Chem.* **1981**, *213*, 351.

(4) Colbran, S. B.; Lahoz, F. J.; Raithby, P. R.; Lewis, J.; Johnson, B. F. G.; Cardin, C. J. *J. Chem. Soc., Dalton Trans.* **1988**, 173. Ciani, G.; Graslascelli, L.; Sironi, A. *J. Chem. Soc., Chem. Commun.* **1981**, 563. Vidal, J. L.; Fiato, R. A.; Cosby, L. A.; Pruett, R. L. *Inorg. Chem.* **1978**, *17*, 2574.

(5) Thompson, R. *Prog. Boron Chem.* **1970**, *2*, 173.

(6) Evidence for a cobalt boride has been published. Schmid, G.; Bätzel, V.; Etzrodt, G.; Pfeil, R. *J. Organomet. Chem.* **1975**, *86*, 257.

(7) Wong, K. S.; Scheidt, W. R.; Fehlner, T. P. *J. Am. Chem. Soc.* **1982**, *105*, 1111. Fehlner, T. P.; Housecroft, C. E.; Scheidt, W. R.; Wong, K. S. *Organometallics* **1983**, *2*, 825.

(8) Rath, N. P.; Fehlner, T. P. *J. Am. Chem. Soc.* **1987**, *109*, 5273.

(9) Tachikawa, M.; Muettterties, E. L. *J. Am. Chem. Soc.* **1980**, *102*, 4541. Beno, M. A.; Williams, J. M.; Tachikawa, M.; Muettterties, E. L. *J. Am. Chem. Soc.* **1981**, *103*, 1485.

(10) Harpp, K. S.; Housecroft, C. E.; Rheingold, A. L.; Shongwe, M. S. *J. Chem. Soc., Chem. Commun.* **1988**, 965. Housecroft, C. E.; Shongwe, M. S.; Rheingold, A. L. *Organometallics* **1988**, *7*, 1885.

(11) Rath, N. P.; Fehlner, T. P. *J. Am. Chem. Soc.* **1988**, *110*, 5345.

(12) Curiously, the reaction of  $[\text{Rh}(\text{CO})_2(\text{CH}_3\text{CN})_2]^+$  with the mono- or dianion of **1** does not yield a boron- and metal-containing product.

(13)  $^{11}\text{B}$  NMR (THF, 20 °C) (*cis* isomer)  $\delta$  205 (t,  $^1J_{\text{RhB}} = 23.3$  Hz).

(14) The PPN salt is very dark brown and is soluble in THF,  $\text{Et}_2\text{O}$ ,  $\text{CH}_2\text{Cl}_2$ . FAB MS,  $p^-$  889, 1 boron; IR ( $\text{Et}_2\text{O}$ ,  $\text{cm}^{-1}$ ) 2040 vw, sh, 2013 s, sh, 2008 vs, 1980 w, 1955 w, br;  $^{11}\text{B}$  NMR (THF, 20 °C) (*trans* isomer)  $\delta$  211 (t,  $^1J_{\text{RhB}} = 25.8$  Hz).

(15) Churchill, M. R.; Wormald, J. *J. Chem. Soc., Dalton Trans.* **1974**, 2410.

(16) The  $^{11}\text{B}$  nucleus relaxes mainly by a quadrupolar mechanism, and normal line widths in ferraboranes range from 50 to 250 Hz.<sup>11</sup> As the relaxation rate increases with the charge asymmetry at the nucleus, it is only for very symmetrical environments that narrow lines are observed. Kidd, R. G. *NMR of Newly Accessible Nuclei*; Laszlo, P., Ed.; Academic: New York, 1983; Vol. 2, p 50.

two equivalent rhodium atoms to be observed.<sup>17</sup> These data are consistent with a hexametal carbonyl cluster containing an interstitial boron for which two isomeric structures (Chart I) are possible. The spectroscopic observation of two hexametal products<sup>13,14</sup> demonstrates the production of both cis and trans isomers; however, the data does not definitively identify the most stable isomer.

To confirm the analysis and determine the structure of the most stable isomer,<sup>14</sup> a single-crystal X-ray diffraction study of the PPN (bistriphenylphosphineiminium) salt of the final product was carried out.<sup>18</sup> The structure is shown in Figure 2 and contains a distorted octahedral frame of two Rh(CO)<sub>2</sub> groups and four Fe(CO)<sub>3</sub> groups encapsulating a boron atom. The arrangement with Rh atoms in trans positions is the most stable structure. There are four short Rh-Fe bonds, av 2.730 (2) Å, and four longer Rh-Fe bonds, av 2.884 (2) Å. The longer bonds are bridged by semibridging CO groups: CO(13) and CO(15) to Rh(1) and CO(7) and CO(9) to Rh(2). The Fe-Fe distances, av 2.752 (2) Å, are normal and regular. The CO groups of each trans pair of iron atoms are eclipsed, while the rhodium pair is staggered. In the isoelectronic cluster, [Fe<sub>6</sub>(CO)<sub>16</sub>C]<sup>2-</sup>, the Fe-Fe distances are in two groups, 2.66 (1)-2.74 (1) Å for unbridged bonds and 2.58 (1)-2.63 (1) Å for  $\mu$ -CO bridged bonds;<sup>15</sup> this relationship is opposite to what we find for *trans*-[Fe<sub>4</sub>Rh<sub>2</sub>(CO)<sub>16</sub>B]<sup>-</sup>. Also in the all-iron analogue, the semibridging CO groups are much nearer to a symmetrical displacement. The metal-boron distances are av Rh-B, 2.03 (1) Å, and av Fe-B, 1.94 (1) Å.

The new boride, [Fe<sub>4</sub>Rh<sub>2</sub>(CO)<sub>16</sub>B]<sup>-</sup>, is directly related to the known closed carbide anion [Fe<sub>6</sub>(CO)<sub>16</sub>C]<sup>2-</sup> and thus constitutes another example of a metallaborane analogue of an organometallic species.<sup>15,19</sup> The boride is related in an isolobal sense to the carborane C<sub>2</sub>B<sub>4</sub>H<sub>6</sub> with *cis*-[Fe<sub>4</sub>Rh<sub>2</sub>(CO)<sub>16</sub>B]<sup>-</sup> being analogous to 1,2-C<sub>2</sub>B<sub>4</sub>H<sub>6</sub> and *trans*-[Fe<sub>4</sub>Rh<sub>2</sub>(CO)<sub>16</sub>B]<sup>-</sup> to 1,6-C<sub>2</sub>B<sub>4</sub>H<sub>6</sub>. As the formation of *cis*-[Fe<sub>4</sub>Rh<sub>2</sub>(CO)<sub>16</sub>B]<sup>-</sup> is rapid with respect to its isomerization to *trans*-[Fe<sub>4</sub>Rh<sub>2</sub>(CO)<sub>16</sub>B]<sup>-</sup>, we have been able to study the kinetics of the interconversion.<sup>20</sup> While a discussion of the results is not possible in this communication, a comparison of the isomerization rate with that of 1,2-C<sub>2</sub>B<sub>4</sub>H<sub>6</sub> is worth noting.<sup>21,22</sup> From the Arrhenius parameters for the isomerization of the boride and the stated conditions for the isomerization of the carborane,<sup>21</sup> we estimate that the transition-metal boride isomerizes 3 × 10<sup>4</sup> times faster than the carborane at 250 °C. The more facile rearrangement of the transition-metal system is expected. Note that if the formation of [Fe<sub>4</sub>Rh<sub>2</sub>(CO)<sub>16</sub>B]<sup>-</sup> had been slow with respect to isomerization or if only crystalline products had been characterized, *trans*-[Fe<sub>4</sub>Rh<sub>2</sub>(CO)<sub>16</sub>B]<sup>-</sup> would have been the sole product observed. Hence, in transition-metal cluster systems it is risky to base mechanistic conclusions on cluster product structure alone.<sup>23</sup>

(17) Assuming the relationship between  $J_{\text{RHB}}$  and  $J_{\text{RHC}}$  will be similar to that between  $J_{\text{BH}}$  and  $J_{\text{CH}}$  the observed  $J_{\text{RHB}}$  coupling constant is consistent with the range observed for  $J_{\text{RHC}}$ . Onak, T.; Leach, J. B.; Anderson, S.; Frisch, M. J. *J. Magn. Reson.* **1976**, *23*, 237. Brevard, C.; Granger, P. *Handbook of High Resolution Multinuclear NMR*; Wiley: New York, 1981; p 158.

(18) Crystal data: C<sub>2</sub>H<sub>30</sub>BNO<sub>16</sub>P<sub>2</sub>Fe<sub>4</sub>Rh<sub>2</sub>, monoclinic,  $P2_1/c$ ,  $a = 11.554$  (4) Å,  $b = 16.007$  (6) Å,  $c = 30.464$  (13) Å,  $\beta = 97.11$  (3)°,  $U = 5590$  Å<sup>3</sup>,  $Z = 4$ ,  $\mu(\text{Mo K}\alpha) = 17.2$  cm<sup>-1</sup>,  $D(\text{calcd}) = 1.66$  g cm<sup>-3</sup>,  $T = 293$  K, black specimen,  $0.22 \times 0.26 \times 0.31$  mm. Of 6442 data collected (Nicolet R3m,  $4^\circ \leq 2\theta \leq 42^\circ$ ) and corrected for absorption, 6017 were independent, and 3846 were observed ( $5\sigma F_o$ ). Disorder in the Fe<sub>4</sub> plane of the anion exists as a low occupancy (~10%) alternative orientation for the four Fe atoms at a ~45° rotation about the Rh-Rh axis. Only the metal atom positions for the alternative position were incorporated in the disorder model. With all phenyl rings constrained to rigid, planar hexagons and all non-hydrogen atoms except for the minority Fe positions anisotropic:  $R(F) = 4.28\%$ ,  $R(wF) = 4.63\%$ ,  $\text{GOF} = 1.202$ ,  $N_o/N_v = 6.2$ ,  $\Delta(\rho) = 0.39$  e Å<sup>-3</sup>.

(19) Grimes, R. N. *Acc. Chem. Res.* **1983**, *16*, 22. Kennedy, J. D. *Prog. Inorg. Chem.* **1984**, *32*, 519. Housecroft, C. E.; Fehlner, T. P. *Adv. Organomet. Chem.* **1982**, *21*, 57. Housecroft, C. E. *Polyhedron* **1987**, *6*, 1935. Fehlner, T. P. *N. J. Chem.* **1988**, *12*, 307.

(20) Other examples of cluster isomerization are known. See, for example: Horwitz, C. P.; Shriver, D. F. *J. Am. Chem. Soc.* **1985**, *107*, 8147.

(21) Onak, T.; Drake, R. P.; Dunks, G. B. *Inorg. Chem.* **1964**, *3*, 1686.

(22) McKee, M. L. *J. Am. Chem. Soc.* **1988**, *110*, 5317.

(23) For a related example, see: Barreto, R. D.; Fehlner, T. P. *J. Am. Chem. Soc.* **1988**, *110*, 4471.

**Acknowledgment.** The support of the National Science Foundation is gratefully acknowledged.

**Supplementary Material Available:** Tables of atom coordinates, bond distances and angles, and anisotropic thermal parameters (12 pages); tables of observed and calculated structure factors (23 pages). Ordering information is given on any current masthead page.

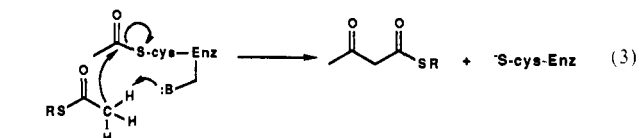
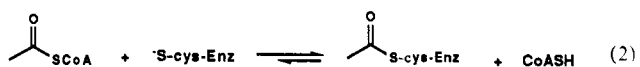
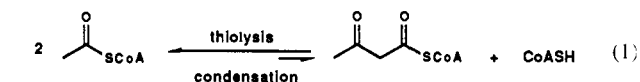
### Bio-Claisen Condensation Catalyzed by Thiolase from *Zoogloea ramigera*. Active Site Cysteine Residues

Satoru Masamune,\*<sup>1</sup> Michelle A. J. Palmer,<sup>1</sup> Remo Gamboni,<sup>1</sup> Stuart Thompson,<sup>1</sup> Jeffrey T. Davis,<sup>1</sup> Simon F. Williams,<sup>1</sup> Oliver P. Peoples,<sup>2</sup> Anthony J. Sinskey,<sup>2</sup> and Christopher T. Walsh<sup>1,3</sup>

Departments of Chemistry and Biology  
Massachusetts Institute of Technology  
Cambridge, Massachusetts 02139

Received October 21, 1988

The enzyme acetoacetyl-CoA thiolase (acetyl-CoA: acetyl-CoA C-acetyl transferase EC 2.3.1.9) is a ubiquitous enzyme.<sup>4</sup> Our recent success in overproducing the biosynthetic thiolase from *Zoogloea ramigera* has facilitated the preliminary characterization and mechanistic investigation of this homotetrameric enzyme, the first thiolase of established primary structure (subunit, 392 a.a.).<sup>5</sup> Thiolase catalyzes the condensation of two acetyl-CoA (AcSCoA) molecules to acetoacetyl-CoA (AcAcSCoA) (eq 1) via two steps. In the first half reaction (eq 2), the active site cysteine attacks AcSCoA to form an acetyl-S-enzyme intermediate and in the second half reaction (eq 3) this intermediate reacts with the anion



formed from the second acetyl-CoA molecule by enzymic deprotonation to complete the condensation. Herein we present evidence to demonstrate that the two cysteine residues, Cys-89 and -378, are essential for the first and second half reactions, respectively. The latter represents the catalytic base that has been sought after since Lynen's original proposal of the above mechanism in 1953.<sup>6</sup> A third cysteine residue (Cys-125) has also been found to be located close to Cys-89, and thus three of the total five cysteines (89, 125, 324, 378, 388) of the enzyme are in or near the active site.

**Acetyl-S-enzyme Involving Cys-89.** As described earlier,<sup>14</sup> C-iodoacetamide reacts with Cys-89 and inactivates the enzyme

(1) Department of Chemistry.

(2) Department of Biology.

(3) Present address: Department of Biological Chemistry and Molecular Pharmacology, Harvard Medical School, Boston, Massachusetts 02115.

(4) Davis, J. T.; Moore, R. N.; Imperiali, B.; Pratt, A. J.; Kobayashi, K.; Masamune, S.; Sinskey, A. J.; Walsh, C. T.; Fukui, T.; Tomita, K. *J. Biol. Chem.* **1987**, *262*, 82 and references quoted therein.

(5) (a) Peoples, O. P.; Masamune, S.; Walsh, C. T.; Sinskey, A. J. *J. Biol. Chem.* **1987**, *262*, 97. (b) Peoples, O. P.; Sinskey, A. J. *Eur. J. Biochem.*, to be submitted. (c) Davis, J. T.; Chen, H.-H.; Moore, R. N.; Nishitani, Y.; Masamune, S.; Sinskey, A. J.; Walsh, C. T. *J. Biol. Chem.* **1987**, *262*, 90.

(6) (a) Lynen, F. *Federation Proc.* **1953**, *12*, 683. Also see: (b) Gehring, U.; Harris, J. I. *FEBS Lett.* **1968**, *1*, 150. (c) Gehring, U.; Riepertinger, C.; Lynen, F. *Eur. J. Biochem.* **1968**, *6*, 264. (d) Gilbert, H. F. *Biochemistry* **1981**, *20*, 5643. (e) Gilbert, H. F.; Lennox, B. J.; Mossman, C. D.; Carle, W. C. *J. Biol. Chem.* **1981**, *256*, 7371.